Tom Milligan
Milligan & Associates
8204 West Polk Place
Littleton, CO 80123
(303) 977-7268
(303) 977-8853 (Fax)
TMilligan@leee.org (e-mail)

A Novel UWB Feeding Mechanism for the TEM Horn Antenna, Reflector IRA, and the Vivaldi Antenna

Majid Manteghi and Yahya Rahmat-Samii

Electrical Engineering Department, University of California, Los Angeles
Los Angeles, California 90095-1594 USA
E-mail: majid@ee.ucla.edu, rahmat@ee.ucla.edu

Keywords: Antenna feeds; reflector antenna feeds; antenna transient analysis; horn antennas; Vivaldi antennas; ultra-wideband; impulse radiating antennas; baluns

1. Introduction

Balanced antennas are an important class of radiation structures; however, interference and shielding considerations usually restrict the designs to using balanced transmission lines at high frequencies. Feeding a balanced antenna with an unbalanced transmission line has been always an issue for antenna designers [1, 2]. Sometimes, designing a proper balanced-to-unbalanced transformer (balun) is as complicated as designing the antenna itself. For balanced ultra-wideband (UWB) impulse-radiating antennas (IRA), this is even more complicated due to their phase linearity and multi-octave frequency bandwidth. Tapered baluns have been used for Vivaldi and transverse electromagnetic (TEM) horn antennas [3]. The size of the tapered balun should be at least of the order of the wavelength of the lowest frequency. At higher frequencies, this tapered balun is long enough to produce some radiation losses; furthermore, it increases the antenna system total size and cost.

This paper proposes a method for feeding a balanced IRA with an unbalanced transmission line. This method is based on the current distribution on the surface of the antenna. The Method of Moments (MoM) simulations show that for the IRAs, there are some areas with low current density in comparison to the current density of the feeding points, almost over the entire frequency range. The coaxial cable is attached to the antenna's body all the way from the feeding point to an area of low current density, and extends out of the antenna structure at that point. This tremendously reduces the current density on the body of the coaxial cable. As a result, the current balance between two parts of the antenna is not disturbed. This method is applied to the TEM horn antenna, the reflector IRA, and the Vivaldi antenna. Some earlier empirical observations on the spiral antenna showed that the body of the antenna can be used to omit the balun in the antenna design [4]. Also, a point on the antenna's body with zero potential has been considered as a natural balun [5] for a coaxial-cable feeding of a folded dipole.

2. Balanced Antennas

A balanced antenna usually has at least one potential symmetry plane, which can be grounded due to the symmetric structure. For example, for a dipole antenna this plane crosses the antenna axis at the feeding point and divides it into two poles. The goal is to feed the antenna in such a way that these two poles have exactly the same current distributions (even symmetry).

If one feeds a balanced antenna using a balanced source right at the feeding point, then due to the symmetric structure the current will have an even symmetry, and the antenna will be fed properly (Figure 1a). This is not always possible, so we usually have to use

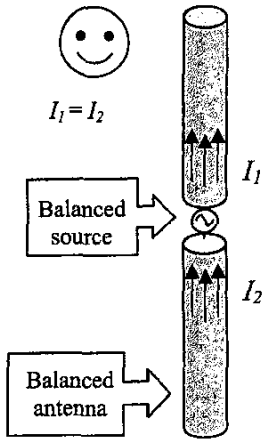

Figure 1a. A balanced antenna is fed by a balanced source at the feeding point.

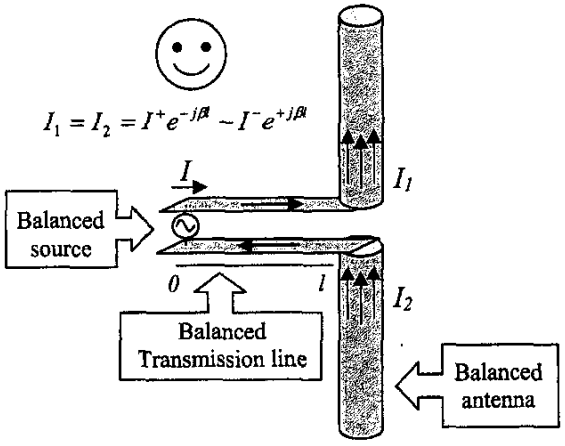

Figure 1b. A balanced antenna is fed by a balanced source through a balanced transmission line.

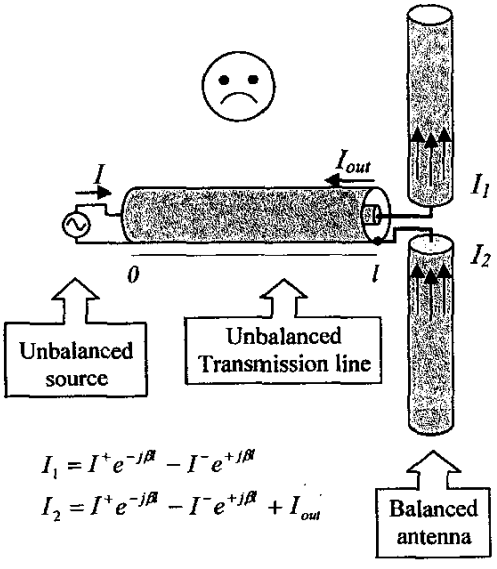

Figure 1c. A balanced antenna is fed by an unbalanced source through an unbalanced transmission line.

transmission lines to deliver the power to the antenna. A second choice is using a balanced source and a balanced transmission line to feed the antenna. Again, all components are balanced and the current has to have even symmetry so that the current distributions have an even symmetry (Figure 1b). Unfortunately, balanced sources and transmission lines are leaky at higher frequencies, and we have to use shielded sources and unbalanced coaxial cables as a feeding network.

Assume that the power generated by an unbalanced source is delivered to the antenna by a coaxial cable. The inner connector of the coaxial cable is connected to one pole of the balanced antenna, and the cladding is connected to the other pole (Figure 1c). One can write the Kirchhoff's current law as

$$I_1 = I^+e^{-j\beta l} - I^-e^{+j\beta l},$$
$$I_2 = I^+e^{-j\beta l} - I^-e^{+j\beta l} + I_{out}, \quad (1)$$

where I^+ is the forward current, I^- is the reflected current, and I_{out} is the current on the outer layer of the coaxial cable. The reference plane is at the junction of the source and the coaxial cable, l is the length, and β is the propagation constant of the coaxial cable. This simple model shows that if $I_{out} \neq 0$, then $I_1 \neq I_2$, and it indicates that the antenna is not fed in a symmetric way. Unbalanced current on the antenna's body will generate an asymmetric E-plane far-field pattern. Also, the current on the outer layer of the coaxial cable usually radiates in an improper direction and with improper polarization. To avoid this problem, one has to force I_{out} to be equal to zero.

A balun is conventionally used to force $I_1 = I_2$ for many different antennas. For impulse-radiating antenna applications, a balun has to have the following properties:

- Balanced currents on both parts of the antenna in the entire frequency band
- Match at the input and output in the entire frequency band
- Linear phase (no phase distortion)
- Low loss
- Low profile
- Low price

Meeting these requirements sometimes makes the balun design as complicated as the antenna design itself. The method proposed in this paper is based on using the antenna's body as part of the feeding structure to avoid the balun design. The idea is to find a low-current-density point on the antenna's body, using simulation tools; to attach the coaxial cable to the antenna's body up to that point; and to extend the cable out of the antenna's body there. This will guarantee that even if there is some current on the outer layer of the coaxial cable, it would be a small current, and it will not change the balance between the current on the antenna's two poles. A dummy cable can be used on the other part of the antenna to make the structure more symmetric. This method of feeding has been investigated for a TEM horn antenna, a Vivaldi antenna, and a reflector IRA. The details of measured and simulated results for the above-mentioned antennas will be discussed in the next parts.

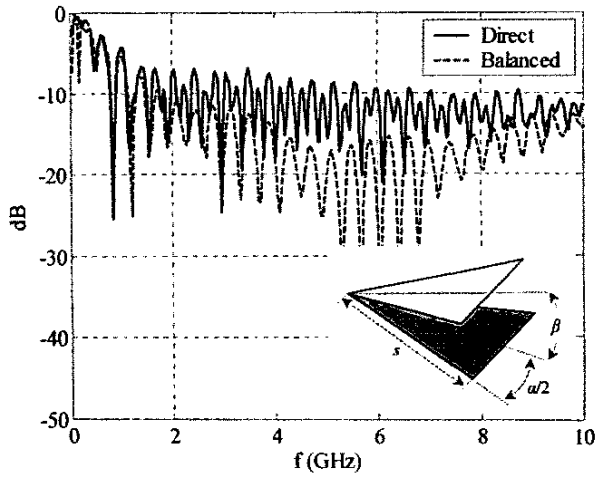

Figure 2. The measured reflection coefficient of the TEM horn antenna for a direct and a balanced feed. The geometry of the TEM horn antenna and its dimensional parameters are also shown.

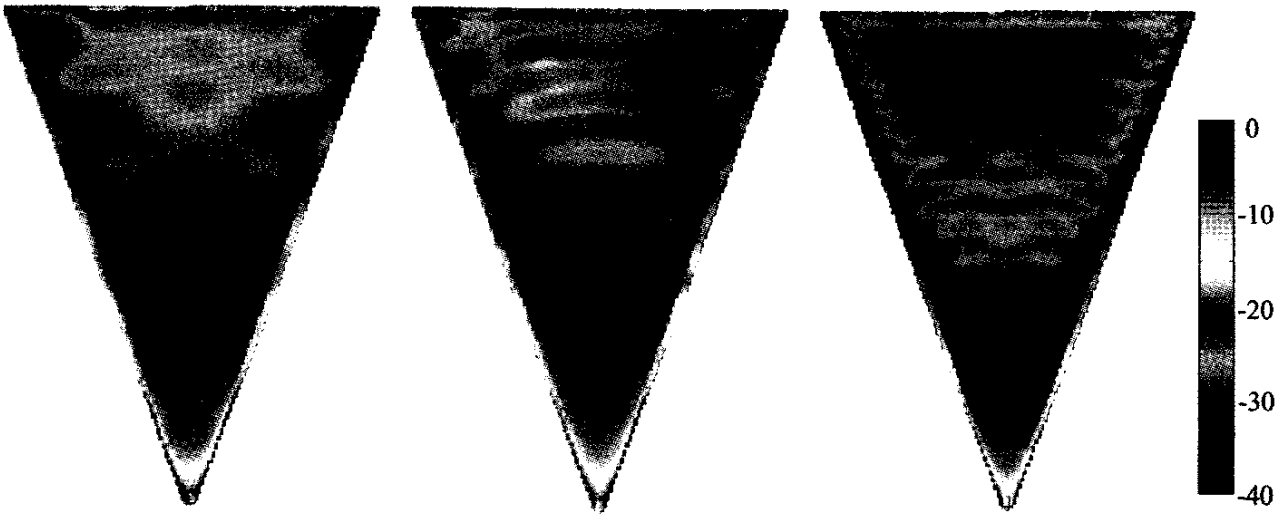

Figure 3. The calculated current distributions on one of the TEM horn antenna's arms at (l-r) 2 GHz, 4 GHz, and 7 GHz.

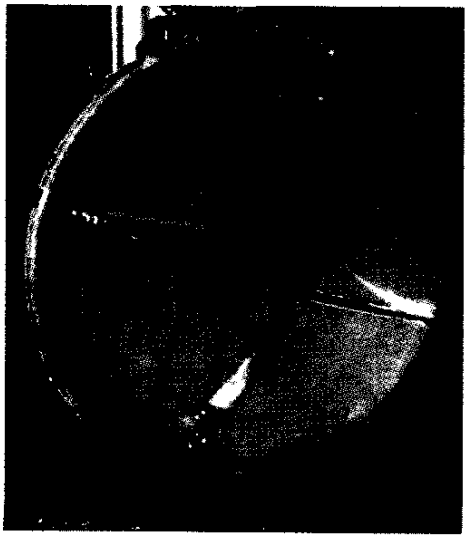

Figure 6a. The UCLA 60 cm reflector impulse-radiating antenna (IRA).

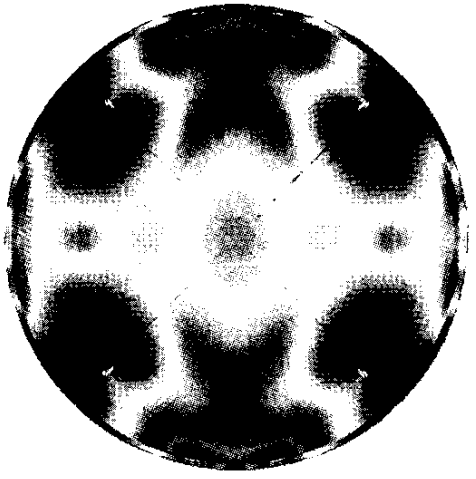

Figure 6b. The calculated current distribution on the surface of the IRA at 2 GHz.

3. TEM Horn Antenna

The TEM horn antenna is one of the most popular antennas for impulse-radiating applications, due to its low phase distortion and wide frequency bandwidth [6]. The basic form of the TEM horn antenna consists of two triangular conductors, of side length s, with the angle at the apex being α, forming a "V" structure with an angle of β (Figure 2). Because of the balanced structure, either a balanced transmission line (for example, the parallel-plate transmission line) or an unbalanced transmission line (a coaxial cable) with an ultra-wideband balun is needed to feed the antenna. For the TEM horn antenna used in this work, the values $\alpha = 40°$, $\beta = 20°$, and $s = 42.7$ cm were chosen, in order to have $Z_{in} = 100\,\Omega$ [7]. The UCLA Hybrid EFIE and MFIE Iterative (HEMI) [8] Method of Moments (MoM) software was used to simulate the antenna, with a balanced source located at the center of the wire that connects the apex of the upper triangle to the lower triangle. Figures 3a, 3b, and 3c show the calculated current distributions on the antenna's body at 2 GHz, 4 GHz, and 7 GHz, respectively. As one can see from these figures, there is a high current density at the feeding point and edges. There are some areas far from these high-current-density parts that carry low current densities for almost the entire frequency band. These simulations show that the proper point to detach the coaxial cable is somewhere inside that low-current-density area. First, the antenna was fed by a coaxial cable directly at the feeding point (an unbalanced transmission line is connected directly to the balanced antenna), and then the coaxial cable was attached to one of the triangular conductors and extended out at a low-current-density point. Figure 4 shows the TEM horn antenna constructed at UCLA with its balanced feed. The measured E-plane far-field patterns for this antenna, both with an unbalanced and a balanced feed and excited at 2 GHz and 4 GHz, are shown in Figures 5a and 5b. These figures show that the antenna with a balanced feed had a more symmetric far-field pattern. The reflection coefficients of the antenna for the two feeding structures were somewhat different: this was due to the differences in current distribution for the direct and balanced feeding structures (Figure 2).

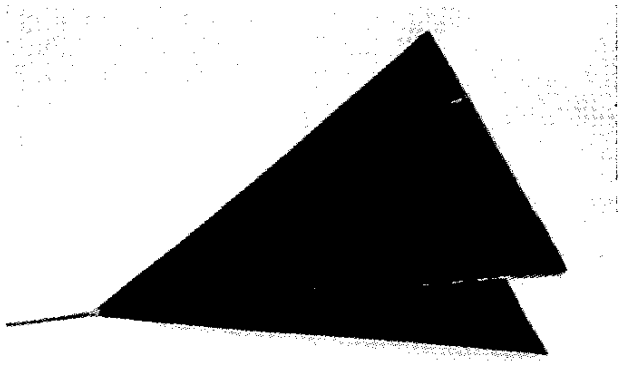

Figure 4a. The TEM horn antenna with the direct feed.

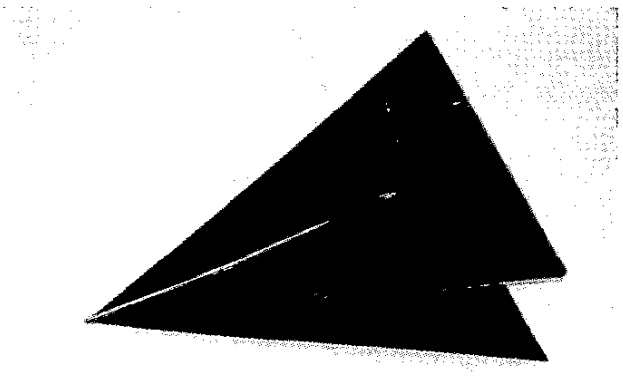

Figure 4b. The TEM horn antenna with the balanced feed. The coaxial cable is attached to one of the antenna's triangles up to a point with low current density.

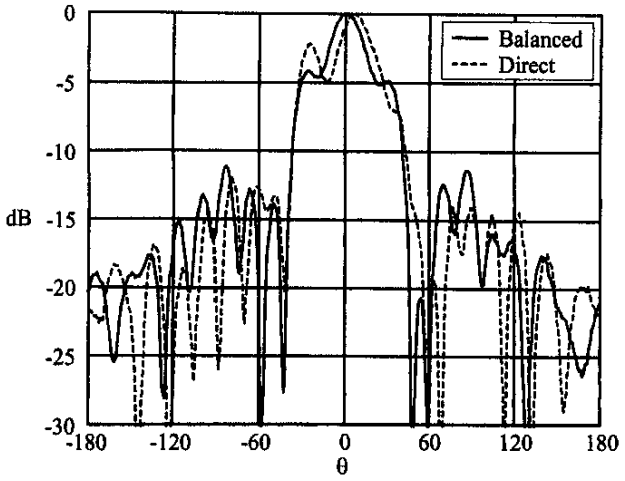

Figure 5a. The measured far-field patterns of the TEM horn antenna with both an unbalanced and a balanced feed at 2 GHz.

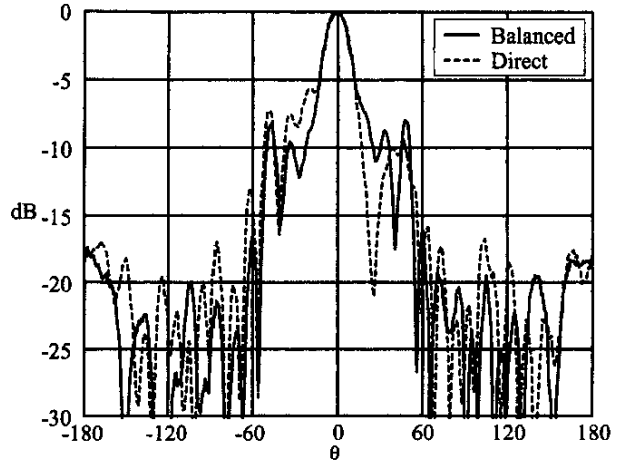

Figure 5b. The measured far-field patterns of the TEM horn antenna with both an unbalanced and a balanced feed at 4 GHz.

4. Reflector IRA

A nondispersive TEM feed structure is employed to illuminate a parabolic reflector to realize a reflector impulse-radiating antenna (IRA) [9, 10]. In ideal circumstances, the parabolic reflector converts the spherical TEM mode on the feeding structure

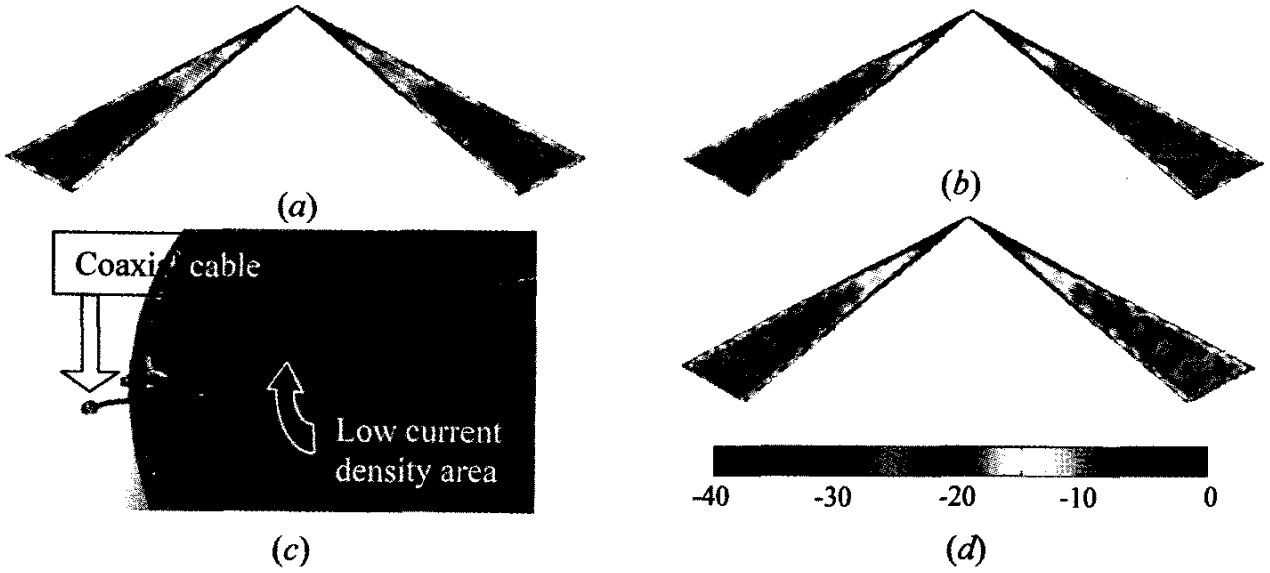

Figure 7. The calculated current density on the TEM feed of the reflector IRA at (a) 2 GHz, (b) 4 GHz, and (d) 6 GHz. (c) The attachment of the coaxial cable to the reflector IRA in a low-current-density area.

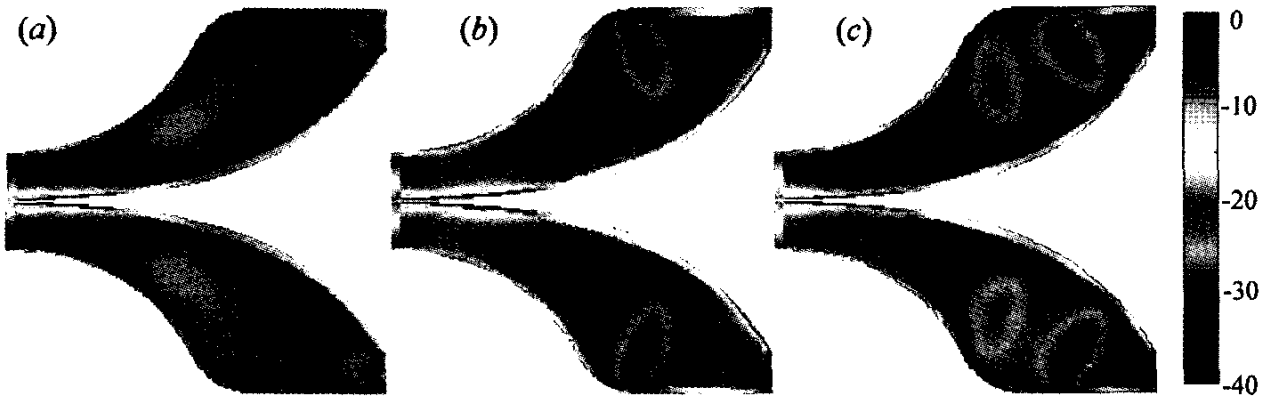

Figure 9. The calculated current distributions on one of the Vivaldi antenna's arms at (a) 2 GHz, (b) 4 GHz, and (c) 6 GHz.

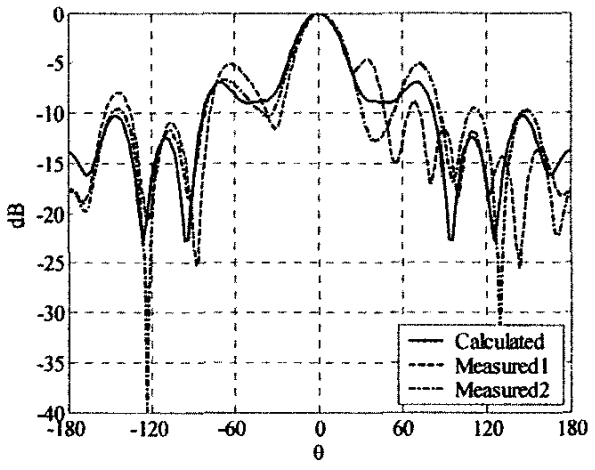

Figure 11a. The calculated and measured E-plane far-field patterns of the Vivaldi antenna at 4 GHz. The Vivaldi antenna with a direct feed has an asymmetric radiation far-field pattern, but the antenna with a balanced feed has a much more symmetric far-field pattern.

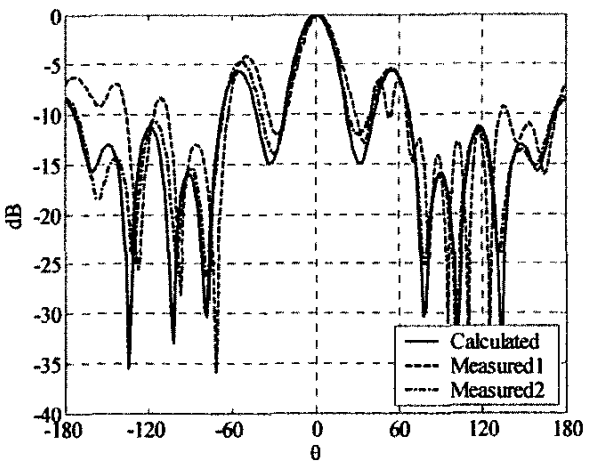

Figure 11b. The calculated and measured E-plane far-field patterns of the Vivaldi antenna at 6 GHz. The Vivaldi antenna with a direct feed has an asymmetric radiation far-field pattern, but the antenna with a balanced feed has a much more symmetric far-field pattern.

to a uniform-phase plane wave at the aperture of the reflector. An ultra-wideband balun is needed to connect the balanced TEM feed to an unbalanced transmission line.

The reflector IRA constructed at UCLA, shown in Figure 6a, consisted of a 60 cm reflector and a 90° conically symmetric balanced TEM transmission-line feed. The HEMI software was employed to calculate the antenna's surface currents and the far-field characteristics. The model used for the MoM calculation was fed by a balanced source at the focal point. The simulation results for the antenna's current distribution at 2 GHz is shown in Figure 6b. Figures 7a, 7b, and 7d demonstrate that the current density on the coplanar feed decreased with distance from the focal point. Also, a standing-wave effect at the end of the feeding arms could be seen. Furthermore, the calculated currents showed that the current density was higher at the edges of the excitation arms, and had lower density along the middle of each arm. The points with lowest current density on the feeding arms were the right places for the coaxial cable to detach from the arms (Figure 7c). Therefore, we could use each one of these arms as an ultra-wideband balun. The calculated and measured far-field patterns of the antenna are shown in Figures 8a and 8b at 2 GHz and 4 GHz, respectively. The measured symmetric far-field patterns confirmed that the antenna had a balanced feed.

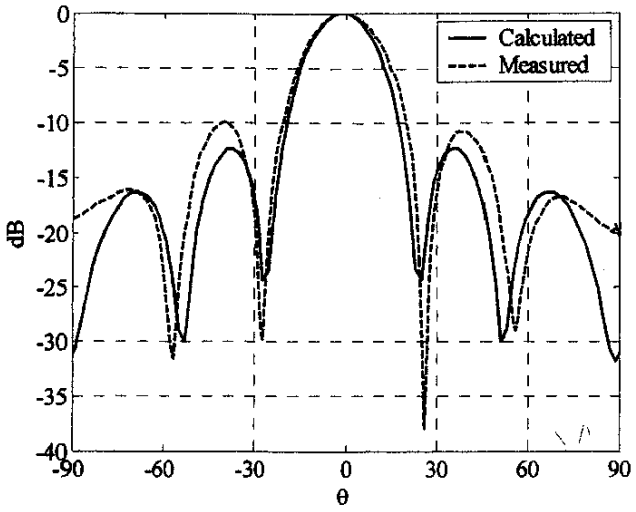

Figure 8a. The calculated and measured IRA E-plane far-field patterns at 2 GHz. Both the calculated and the measured results show symmetric behavior around $\theta = 0°$.

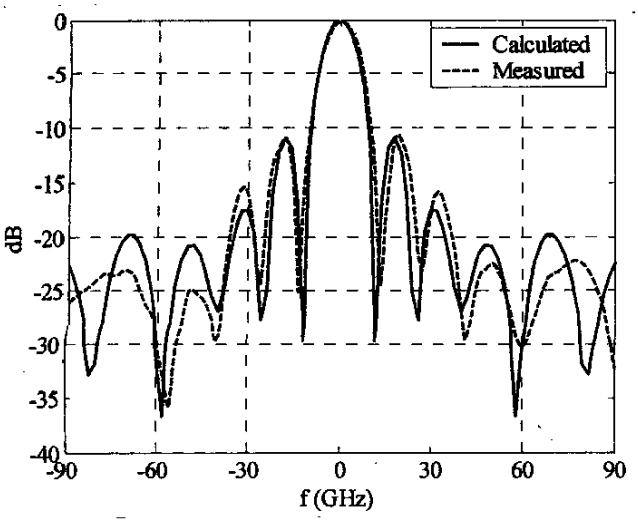

Figure 8b. The calculated and measured IRA E-plane far-field patterns at 4 GHz. Both the calculated and the measured results show symmetric behavior around $\theta = 0°$.

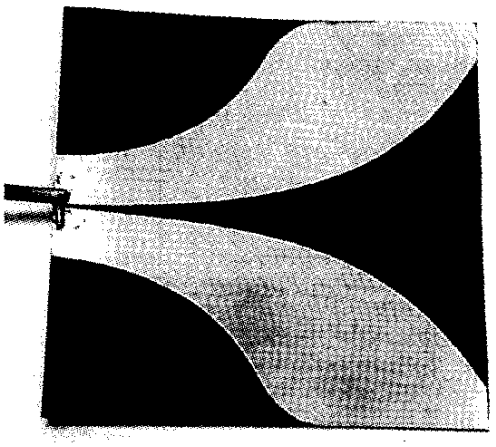

Figure 10a. The Vivaldi antenna with a direct feed.

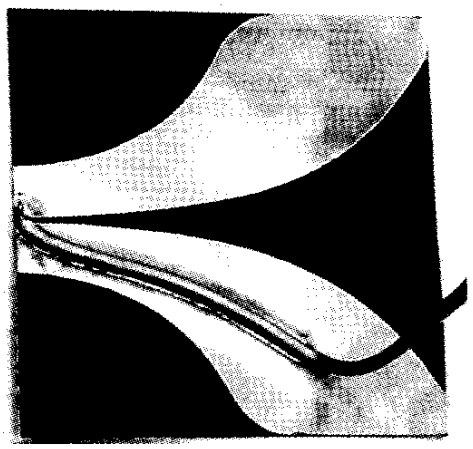

Figure 10b. The Vivaldi antenna with a feed using with current-distribution considerations.

5. Vivaldi Antenna

It has been shown that an open-ended tapered slot line is a broadband traveling-wave end-fire antenna [11, 12, 13]. The early designs of the Vivaldi antenna were balanced structures, and therefore had to be fed by an ultra-wideband balun. However, newer designs use double-sided arms and a stripline feed to eliminate the balun [14, 15]. There are still some portions of the antenna's body that function as a balun and that do not contribute to the radiation. This antenna has been chosen as an ultra-wideband balanced antenna to inspect the accuracy of our feeding method.

A slot with a length of 100 mm, starting from a width of 0.7 mm, and expanding exponentially to a width of 80 mm at the

end, was printed on a piece of 100 mm × 100 mm RT-Duroid ($\varepsilon_r = 2.2$ and h=0.245 mm). The substrate was chosen as thin and with as low an ε_r as possible in order to have the free-space condition. The model that was used with the HEMI software did not contain the dielectric. This simulation model was fed at the beginning of the narrow side of the slot with a balanced source located at the center of a wire connecting one arm to the other arm. The calculated current distributions at 2 GHz, 4 GHz, and 6 GHz are shown in Figures 9a, 9b, and 9c, respectively. These figures show that the current density on the exponentially tapered slotline decreased with distance from the feeding point. Also, the calculated currents showed that the current density was higher at the edges of the slot, and had a lower density along the middle of the wide part of the antenna. The points with low current density on the radiating arms were the right places for the coaxial cable to detach from the antenna's body. This antenna was fed directly with a coaxial cable (Figure 10a) and with current-distribution considerations (Figure 10b). The calculated E-plane far-field pattern is compared with the measured pattern for these two feeding methods in Figures 11a and 11b. One can see from these figures that the balanced-fed antenna had a much more symmetric E-plane far-field pattern than did the antenna fed directly with an unbalanced cable.

6. Conclusion

In this paper, a feeding method for balanced ultra-wideband antennas, using an unbalanced transmission line, was suggested. The TEM horn antenna, the reflector impulse-radiating antenna, and the Vivaldi antenna were chosen as unbalanced antennas, and the method was applied to feed them with a coaxial cable. This method is based on the current distribution on the antenna's body. The simulation results for these antennas show that there are some areas on the antenna's structure that have a low current density compared to the excitation point over the entire frequency range of operation. It was shown in this paper that if the feeding transmission line is attached to the antenna's body from the feeding point to a point with low current density, and extended out of the antenna body at that point, the far-field pattern will still be symmetric, as if the antenna had been fed by a balanced transmission line.

The TEM horn antenna was simulated using the *HEMI* software, and was fed by an unbalanced coaxial cable, both directly at the feeding point and using this method. The measured results and the simulation results showed that our feeding method resulted in a great improvement in comparison with the direct-feeding method.

This method was also applied to the reflector impulse-radiating antenna. The simulation results for a balanced source were compared with the measured results, and showed good agreement. Also, the Vivaldi antenna was fed both by considering the low-current-density area and direct feeding. The E-plane far-field pattern of the new feeding method had good agreement with the result generated by the HEMI software for a balanced-fed antenna.

7. References

1. G. Oltman, "The Compensated Balun," *IEEE Transactions on Microwave Theory and Techniques*, **MTT-8**, 6, November 1960, pp. 672-673.

2. J. H. Craven, "A Novel Broad-Band Balun," *IEEE Transactions on Microwave Theory and Techniques*, **MTT-14**, 3, March 1966, pp. 112-119.

3. P. R. Foster and S. M. Tun, "A Wideband Balun from Coaxial Line to TEM Line," *Proceedings of ICAP'95, Ninth International Conference on Antennas and Propagation*, (Conf. Publ. No. 407), **4-7**, April 1995, pp. 286-290.

4. J. D. Dyson, "The Unidirectional Equiangular Spiral Antenna," *IEEE Transactions on Antennas and Propagation*, **AP-7**, 4, October 1959, pp. 329-334.

5. B. A. Munk, "Balun, etc.," in J. D. Kraus and R. J. Marhefka, *Antennas: For All Applications, Third Edition*, New York, McGraw-Hill, 2002, pp. 803-826.

6. R. T. Lee and G. S. Smith, "A Design Study for the Basic TEM Horn Antenna," *IEEE Antennas and Propagation Magazine*, **46**, 1, February 2004, pp. 86-92.

7. R. T. Lee and G. S. Smith, "A Design Study for the Basic TEM Horn Antenna," IEEE International Symposium on Antennas and Propagation *Digest*, **1**, Columbus, Ohio, June 2003, pp. 225-228.

8. R. E. Hodges and Y. Rahmat-Samii, "An Iterative Current-Based Hybrid Method for Complex Structures," *IEEE Transactions on Antennas and Propagation*, **AP-45**, 2, February 1997, pp. 265-276.

9. R. H. DuHamel et al., "Frequency Independent Conical Feeds for Lens and Reflectors," IEEE International Symposium on Antennas and Propagation *Digest*, **6**, September 1968, pp. 414-418.

10. E. G. Farr, C. E. Baum, and C. J. Buchenauer, "Impulse Radiating Antennas, Part II," in L. Carin and L. B. Felsen (eds.), *Ultra Wideband/Short-Pulse Electromagnetics 2*, New York, Plenum Press, 1995, pp. 159-170.

11. P. J. Gibson, "The Vivaldi Aerial," *Proceedings 9th European Microwave Conference*, Brighton, UK, September 1979, pp. 101-105.

12. Joon Shin and D. H. Schaubert, "A Parameter Study of Stripline-Fed Vivaldi Notch-Antenna Arrays," *IEEE Transactions on Antennas and Propagation*, **AP-47**, 5, May 1999, pp. 879-886.

13. B. Stockbroeckx and A. Vander Vorst, "Copolar and Cross-Polar Radiation of Vivaldi Antenna on Dielectric Substrate," *IEEE Transactions on Antennas and Propagation*, **AP-48**, 1, January 2000, pp. 19-25.

14. E. Gazit, "Improved Design of the Vivaldi Antenna," *IEE Proceedings on Microwaves, Antennas, and Propagation*, **135**, 2, April 1988, pp. 89-92.

15. N. Fourikis, N. Lioutas, and N. V. Shuley, "Parametric Study of the Co- and Cross-Polarisation Characteristics of Tapered Planar and Antipodal Slotline Antennas," *IEE Proceedings on Microwaves, Antennas, and Propagation*, **140**, 1, February 1993, pp. 17-22.

Ideas for Antenna Designer's Notebook

Ideas are needed for future issues of the Antenna Designer's Notebook. Please send your suggestions to Tom Milligan and they will be considered for publication as quickly as possible. Topics can include antenna design tips, equations, nomographs, or shortcuts, as well as ideas to improve or facilitate measurements.